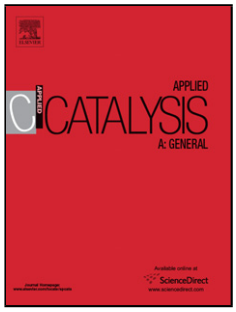

Title: Effect of the surface oxidation of carbon nanotubes on the selective cyclization of citronellal

Author: A.B. Dongil L. Pastor-Pérez J.L.G. Fierro N. Escalona A. Sepúlveda-Escribano

PII: S0926-860X(16)30274-5
DOI: http://dx.doi.org/doi:10.1016/j.apcata.2016.05.021
Reference: APCATA 15885

To appear in: *Applied Catalysis A: General*

Received date: 28-1-2016
Revised date: 13-4-2016
Accepted date: 22-5-2016

Please cite this article as: A.B.Dongil, L.Pastor-Pérez, J.L.G.Fierro, N.Escalona, A.Sepúlveda-Escribano, Effect of the surface oxidation of carbon nanotubes on the selective cyclization of citronellal, Applied Catalysis A, General http://dx.doi.org/10.1016/j.apcata.2016.05.021

Effect of the surface oxidation of carbon nanotubes on the selective cyclization of citronellal

A.B.Dongil [a*], L.Pastor-Pérez[b], J.L.G. Fierro[c] , N.Escalona[d,e], A.Sepúlveda-Escribano[b],

[a] *Universidad de Concepción, departamento de físicoquímica, laboratorio de catálisis por metales, Edmundo Larenas 129, Concepción, Chile.*

[b] *Laboratorio de Materiales Avanzados, Instituto Universitario de Materiales de Alicante, Departamento de Química Inorgánica, Universidad de Alicante, Apartado 99, E-03080 Alicante, Spain*

[c] *Instituto de Catálisis y Petroleoquímica CSIC, Grupo de Energía y Quimica Sostenible, C/Marie Curie2, Cantoblanco, Madrid, Spain*

[d]*Departamento de Ingeniería Química y Bioprocesos, Escuela de Ingeniería, Pontificia Universidad Católica de Chile, Avenida Vicuña Mackenna 4860, Macul, Santiago, Chile.*

[e]*Facultad de Químicas, Pontificia Universidad Católica de Chile.*

To whom correspondence should be addressed

**Dr.* A.B.Dongil*., e-mail:* adongil@udec.cl, *Tel: (56-41) 2207236.*

Graphical abstract

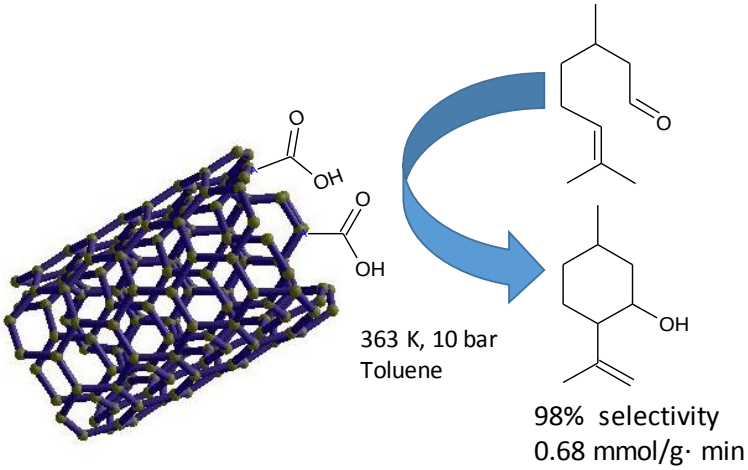

Highlights

- Oxidation of commercial carbon nanotubes in liquid media and air was studied.
- The samples were tested on the cyclization of citronellal.
- The previous ball-milling treatment increases the carboxylic acid concentration.
- The activity is ascribed to the carboxylic groups and the selectivity to isopulegol seems to be related to the pore size.

Abstract

Commercial carbon nanotubes have been oxidized with HNO_3, H_2O_2 and air and they have been tested on the cyclization of citronellal. The materials have been characterized by N_2 adsorption/desorption isotherms, transmission electron microscopy, X-ray diffraction, temperature programmed desorption, potentiometry titration and X-ray photoelectron spectroscopy. The HNO_3-treated samples displayed the largest concentration of carboxylic acids which increased by increasing the oxidation time and by a previous ball-milling treatment. The carboxylic acid groups were found to be the active groups on the reaction and the activity increased by increasing its content. The selectivity to isopulegols was higher (98%) over the most active samples (activity 0.20-0.68 mmol/g·min), which has been explained by their smaller pore size caused by the oxidation treatment. The stability of the most active CNT sample was also proved by recycling the catalyst in 3 cycles.

Keywords: carbon nanotubes; oxidation; ball-milling; citronellal; isomerization; isopulegol.

1. Introduction

Citronellal is a renewable feedstock that can be naturally obtained from a great amount of natural essential oils such as *Cymbopogon nardus* or Java citronella, and it can be used in the chemical industry to replace petroleum in a wide variety of transformations. Among them, the cyclization of citronellal is a relevant reaction in fine chemistry industry as its product, isopulegol, is widely employed in flavor and perfume industry for the production of fragrances and manufacturing menthol, which is an important ingredient in perfumery and pharmaceuticals products [1].

Several heterogeneous catalysts have been studied for the cyclization of citronellal to substitute the environmentally unfriendly Lewis acids ($ZnCl_2$, $AlCl_3$, $SbCl_3$, etc.). Among them, several oxides (SiO_2–Al_2O_3, SiO_2) [2,3], zeolites containing Lewis acid centers, such as Sn and Zr atoms [4] and zirconia-based catalysts [1,5] have been found to be active and selective to certain extent for the reaction. Both Lewis and Brönsted acids have been identified as active sites and, although no precise correlation between acidity and catalytic performance has been established, it has been reported that a proper modulation of the acidity is needed to obtain an optimal activity while avoiding secondary reactions such as condensation, etherification or cracking [6]. Besides acidity, the catalytic performance depends largely on the textural properties of the catalyst and, for example, a comparison between different zeolites and mesoporous materials found that H-MCM-41 offered the best results [6].

In this context, carbon materials arise as excellent candidates given the possibility to control the surface acidity with relatively easy procedures. Moreover, they are chemically stable favouring the deposition of metal nanoparticles in acid and basic media. Their role in catalysis has extensively been reported both as a support and as catalyst its own [7,8].

They can react with multiple molecules to incorporate different heteroatoms (O, N, H, Cl, S, etc.), and the importance of their surface chemistry on a wide variety of reactions has been reviewed [9,10,11]. Besides the surface chemistry it has been proved that the morphology may affect the catalytic performance. Though most of the literature reports the use of activated carbon, mainly due to its high adsorption capacity, for liquid phase reactions a mesoporous material would offer additional advantages. In this sense, still few examples can be found in literature where carbon nanotubes have been used as catalyst its own [12,13,14].

The oxidation of carbon materials and CNT, in particular, has been performed employing several liquid and gas reagents such as H_2SO_4, H_2O_2, HNO_3, NaClO, HCl, ozone, air, etc [15,16]. The type and concentration of surface groups depends on the oxidizer and functionalization conditions [17,18,19,20]. Among the oxidizers, HNO_3 has proved to incorporate a high concentration of oxygen groups while preserving the CNT structure [21]. In general, the oxidation with HNO_3 and H_2O_2 produces acidic materials holding carboxylic acids and, to a smaller extent, lactones, anhydrides and phenol groups. Nonetheless, the obtained amount of oxygen functionalities is larger when HNO_3 is employed [22]. On the other hand, the treatment under air generates a larger proportion of carbonyl and ethers which are neutral or may form basic structures, such as quinone [23].

Therefore, we have explored the effect of different oxidation treatments (HNO_3, H_2O_2 and air) on the surface chemistry of CNT and studied their catalytic performance on the cyclization of racemic citronellal. The effect of the oxidation time with HNO_3 and the previous ball-milling treatment was also evaluated.

2. Experimental

2.1 Oxidation of the CNT

High purity multi-wall carbon nanotubes (i.d. 2–6 nm) were supplied by Nanocyl (Nanocyl 3100, > 95% purity) and submitted to different oxidation treatments. a) CNT were treated with 50 ml/g HNO_3 (65% wt) at 403 K, then they were washed with distilled water until pH ∼7 and dried at 333 K overnight. The oxidation was performed for 24, 16 and 8 h obtaining the samples labeled as CNToxn24, CNToxn16 and CNToxn8 respectively; b) CNToxa: oxidation of CNT under air flow (30 ml/min) at 673 K for 2 h; c) CNToxp: oxidation of CNT with H_2O_2 100 ml/g (30%), at 353 K for 24 h; d) The CNT were submitted to ball milling in a planetary stainless steel Spex 800 rpm for 1 h followed by oxidation as applied for CNToxn8 obtaining the sample CNTmox8; e) Two portions of the sample CNToxn24 were heat-treated in He (50 ml/min) with a heating ramp of 5 K/min at 373 and 473 K for 1 hour and they were labelled as CNToxn24-373 and CNToxn24-473.

2.2 Characterization

Conventional TEM analysis was carried out with a JOEL model JEM-210 electron microscope working at 200 kV and equipped with a INCA Energy TEM 100 analytical system and a SIS MegaView II camera. Samples for analysis were suspended in methanol and placed on copper grids with a holey-carbon film support.

X-ray powder diffraction patterns were recorded on a Rigaku diffractometer equipped with a nickel-filtered CuKα1 radiation (λ= 1.5418˚A), using a $2^{o}\cdot min^{-1}$ scanning rate. N_2 adsorption-desorption analysis was performed at 77 K on a Micromeritics ASAP 2010 apparatus. Specific surface areas were determined via the BET (Brunauer–Emmett–Teller) equation, using adsorption data in the relative pressure range of 0.05–0.3, and pore size distributions were estimated using the BJH model.

The thermogravimetric analyses were performed with a Mettler Toledo Thermogravimetric TGA/SDTA 851 system. The sample was treated under flowing He for 2 h and then heated with a heating rate of 10 $K \cdot min^{-1}$ rate up to 1123 K.

Temperature-programmed desorption (TPD) experiments were carried out in a vertical tube furnace with He as the carrier gas to thermally decompose the stable surface oxygen complexes. 100 mg sample was placed in a quartz tube and heated to 383 K for 1 h, and then the temperature was raised to 1000 K at 10 K min^{-1}.

Acid site concentrations and acid strength measurements of the materials were determined using a potentiometric method [24], whereby a suspension in acetonitrile (Merck, 99.9%) was titrated with *n*-butylamine (Merck, 99%). The variation in electric potential was registered on a Denver Instrument UltraBasic pH/mV meter.

Photoelectron spectra (XPS) were recorded using an Escalab 200 R spectrometer equipped with a hemispherical analyser and using non-monochromatic Mg K X-ray radiation (h = 1253.6 eV). The surface O/C atomic ratios were estimated from the integrated intensities of C 1s and O 1s lines after background subtraction and correction by the atomic sensitivity factors. The spectra were fitted to a combination of Gaussian–Lorentzian lines of variable proportions.

2.3 Reaction

The catalytic performance was tested in a 100 mL stainless steel Parr- type reactor lined with glass at 363 K and 10 bar of He with a stirring speed of 700 r.p.m. For each reaction 50 mg of catalyst, 30 ml of toluene and 0.16 M of racemic citronellal (Sigma Aldrich ≥ 98.0%) was employed. For the recycling studies, 75 mg were initially employed keeping the same reactant concentration and substrate/catalyst ratio. The catalysts were recovered by filtration, extensively washed with acetone and dried under vacuum at 323 K for 6

hours and the amounts of reactant and solvent recalculated according to the catalyst mass recovery. Analyses of reactants and products were followed by gas chromatography mass spectrometry using a GC–MS instrument (Shimadzu GCMS-QP5050) with chiral-Dex 225, a 30-m column (Supelco), and helium as the carrier gas. Small aliquots of sample were taken for analysis by gas chromatography (GC). The activity was calculated as mol converted per minute at 50% conversion and the selectivity was estimated as the sum of all isopulegol isomers divided by the sum of all products formed.

3. Results

3.1 Characterization

In Fig.1 representative TEM images of CNT, CNToxn24 and CNTmox8 are shown. It can be observed that CNT presented quite long tubes with a spatial arrangement that leaves an interstitial space between the nanotubes and that most of the tubes are closed. The images of CNToxn24 suggested a larger proportion of agglomerated tubes compared to CNT and, in general, few open-ends could be detected. On the other hand, for the sample CNTmox8, the images showed that the ball-milling treatment was effective on cutting the nanotubes, though the material also presented a marked proportion of agglomerated tubes compared to CNT. Moreover, barely amorphous carbon was found on the surface of the samples, though the presence of debris formed after nitric acid treatment cannot be disregard as it has been reported previously [25]. These observations were extracted from several TEM images and a selection is included in the supplementary information.

The nitrogen adsorption/desorption isotherms at 77 K of the parent CNT and the modified samples and are shown in Fig.2. The CNT showed the characteristic shape of mesoporous materials with a well-defined hysteresis loop, a noticeable increase of nitrogen adsorption at high relative pressure (0.8–0.9) and barely any nitrogen uptake at low relative pressure.

The isotherms of CNToxa and CNToxp presented similar shape compared to that of the parent CNT but an increase of nitrogen uptake was observed at low relative pressure and a small additional hysteresis loop was developed at medium relative pressures (0.3–0.6). On the other hand, CNTmox8 and CNToxn24 displayed a different profile with much less pronounced hysteresis loop at higher relative pressures. They have also developed a new hysteresis loop at medium relative pressure, more evident than for CNToxa and CNToxp samples, which can be originated by the inner hollow cavity of open-ended CNT created by the treatments [26]. The estimated BET surface area and pore volumes are shown in Table 1. The porosity of the CNT originates from the area at the surface of the tubes, the interstitial space between nanotubes and the inner cavities of the open CNT. As expected, CNT are non-microporous materials and they possess a high specific surface area and a total pore volume above 1 $cm^3\ g^{-1}$, which is primarily due to adsorption on the external surface of the tubes. The oxidation treatment for CNToxa and CNToxp seems to have created micropores, this increasing the surface area. On the other hand, the samples treated with nitric acid displayed similar values of S_{BET}, despite the clear changes on the pore volume which can be explained along with the TEM observations. The chemical and physical treatment may have opened some of the tubes which would increase the surface area and the mesopores volume. However, as the TEM images showed the tubes on CNToxn24 and CNTmox8 were more agglomerated than on the CNT sample and this would in turn decrease the mesopores volume and the S_{BET}. Similar findings have been reported for other wet oxidation treatments [27]. Moreover, the increase in the V micro observed for the HNO_3-treated samples upon increasing the oxidation time can be ascribed to the creation of micropores as suggested for the air and H_2O_2-treated samples. The graphitic order of the materials was evaluated by XRD, and selected patterns are shown in Fig. 3. The parent CNT displayed the characteristic reflections at $2\theta = 26.1\ ^{o}$

and at 2θ = 43.1 º of the (002) and (100) planes of graphite respectively [28]. The XRD patterns of the oxidized samples are similar to that of the parent CNT, this indicating that the structure was preserved after the oxidizing and mechanical treatments.

In Figure 4.a-c the TPD profiles of CO_2 and CO of selected modified samples are shown. The thermogravimetry analyses, in the supplementary information Fig. S2, showed that the as received CNT and CNToxa presented barely any weight loss up to 873 K. Therefore, the H_2O_2 and HNO_3-treated CNT profiles are shown. In Fig. 4a it can be observed the evolution of CO_2 along the temperature range 373-1073 K. All the samples displayed three main peaks with maxima at around 523-593 K, 673-743 K and 823-953 K. These results indicate the presence on the surface of chemical species with different thermal stability, which according to the general criteria proposed in literature would correspond to the desorption of carboxylic acid, carboxylic anhydrides and lactone groups respectively [9,13,29]. The desorption peaks appear at lower temperature for CNToxn24, this indicating a lower thermal stability of those groups, in line with previous works which also reported that by increasing the oxidation time, the decomposition temperature was lower [30,31]. On the other hand, the CO profile in Fig. 4b showed a small peak in the range 673-743 K that matches with the temperature for the second peak observed in the CO_2 profile and corresponds to the decomposition of anhydride groups which are known to originate both CO and CO_2; and a broad peak at higher temperatures with maximum at 953-993 K, this revealing the existence of phenolic and carbonyl/quinone groups [9,13,30]. The intensity of this latter peak was higher for CNToxn16 than CNToxn24 which suggest a larger proportion of C-OH and C=O groups on the former. Furthermore, Fig.4a also shows that by increasing the oxidation time on the HNO_3-treated samples, the intensity of the peak at low temperature corresponding to the decomposition of carboxylic acids increases, as confirmed from the integration, and included in brackets. Moreover,

the desorption at the highest temperature is larger for CNToxn24 than for the other samples, and the sample CNTmox8 displayed the largest peak of evolved CO_2 at low temperature although the oxidation time was 8 hours. The evolved amounts of CO_2 and CO were estimated from the integration of the area under the curves and from them, the oxygen content was also calculated. The results, in Table 2, show that CNTmox8 owns the largest amount of CO_2, CO and O, while CNToxp had the lowest concentration of evolved gases and oxygen. In addition, the oxygen concentration increases upon increasing the oxidation time in agreement with literature [32] except for the sample CNTmox8 which displayed the largest concentration among the samples. This is not surprising considering that the development of oxygen-containing surface groups occurs predominantly at defect sites on the surface and that the ball-milling treatment had created a larger proportion of these reactive sites as the microscopy showed [33]. The estimated amounts of CO_2 and CO for the CNT samples are in quite good agreement with the proposed oxidation mechanism which suggests that the oxidation of carbon materials proceeds *via* introduction of carbonyls followed by their conversion into phenols, carboxylic acids, carboxylic anhydrides and lactones [16]. Although the CO_2/CO ratio has been taken as an indication of the surface acidity, the possible presence of anhydrides on the samples limits its applicability. Therefore, the proportion of carboxylic acid respect to the total oxygen amount was calculated and the values, in Table 2, show that they follow the same trend as those of the total amount of carboxylic acids except for the sample CNToxp which displayed a larger value.

The surface acidity of the materials was estimated from the potentiometric titration curves with *n*-butylamine as the probe molecule. In Table 3 are included the maximum acid strength of the surface sites (derived from the initial electrode potential, $E0$) and the total number of acid sites. The acid strength can be determined according to the criterion

proposed in literature [34]: $E0 > 100$ mV, very strong sites; $0 < E0 < 100$ mV, strong sites; $-100 < E0 < 0$ mV, weak sites; $E0 < -100$ mV, very weak sites. The results confirmed that the parent CNT holds a basic surface and showed that the H_2O_2 and HNO_3-treatment produced very strong acid sites on the CNT, except for the sample CNToxn8 which displayed strong acid sites, whereas CNToxa displayed weak acid sites. As long as the acid density site is concerned, the estimated amount showed that the HNO_3-treated samples displayed similar densities except for the sample previously submitted to milling treatment which showed the largest value. The lowest density of acid sites was measured for the CNT, CNToxa and CNToxp. These results are in line with those obtained by TPD and thermogravimetry, where it is possible to confirm that among the oxidized samples, CNToxa and CNToxp are the materials with the lowest concentration of oxygen–containing functionalities decomposing as CO and CO_2, while in the opposite, CNTmox8 is that with the highest concentration. Moreover, the acid strength correlates quite well with the COOH/O ratio estimated by TPD. These results seem to confirm that the creation of defects sites on CNTmox8, favored the oxidation to carboxylic acid, this increasing the acidity of this sample.

XPS analyses were carried out to assess for the type of functional groups on the prepared samples. The relative amounts of the different species, C and O, were calculated from the corresponding peak areas divided by the sensitivity factors and are shown in Table 4. The O/C ratios obtained showed a moderate increase in the oxygen content for the CNToxa and CNToxp samples compared to the nitric-treated samples and that the samples with the largest O/C ratio were CNTmox8 and CNToxn24. Furthermore, the oxygen concentration on the samples treated with nitric acid increases upon increasing the oxidation time, being more pronounced when the oxidation time increases from 8 to 16 hours in quite good agreement with the data obtained by TPD. In addition, the large O/C

ratio for the CNTmox8 sample, despite the treatment time, showed that the previous milling of the CNT favoured the surface oxidation in line with the TPD results and previous literature [33].

The O 1s region can be deconvoluted in three components to obtain information on the nature of the surface oxygen groups: oxygen in carbonyl and quinone groups (531.4 eV); C-O oxygen in hydroxyl and ether groups (532.6 eV); oxygen in acidic carboxyl groups (534.6 eV) [35]. According to these contributions the resulting proportion of the oxygen components are shown in Table 4. The proportion of the different oxygen species also changes among the samples and it was found that the contribution ascribed to O=C-O follows the same trend as that obtained from the TPD analyses, with CNTmox8 having the largest concentration, and followed by the other HNO_3-treated samples in decreasing order of oxidation time.

3.2 Reaction results

The catalysts were tested in the cyclization of citronellal and the evolution of conversion with time until 240 min. is shown Fig. 5. It was found that only the CNT treated with nitric acid were active. Among them, the best catalyst in terms of activity and selectivity was CNTmox8 which reached 100% conversion at 90 min. of reaction. The estimated activity at 50% conversion is shown in Table 5 and it follows the trend: CNTmox8 > CNToxn24 > CNToxn16 > CNToxn8.

The selectivity to isopulegol achieved at 100% conversion is shown in Table 5, where it is shown that the catalysts CNTmox8, and CNToxn24 were 97-98% selective to isopulegol. The less active catalysts were also the less selective and CNToxn16, CNToxn8 afforded 78 and 69% selectivity respectively. These selectivity values being nearly constant with conversion as shown in Fig. 6. The secondary products were identified as isopulegol ethers, which are generated by condensation of two isopulegol

molecules. In order to assess for the stability of the most active catalyst, CNTmox8 was employed in successive cycles and it was observed that it preserved relatively well the activity as the values in Table 5 show.

The activity obtained with CNTmox8 was lower than that reported for the cyclization of racemic citronellal over H-MCM-41 under similar conditions, though the surface area of the CNT sample is also significantly lower [6]; and the conversion profile was similar to that for sulfatated-ZrO_2/carbon molecular sieve, despite the milder conditions employed in the present study [36]. However, the selectivity to isopulegols over CNTmox8 was higher than the reported in the references which was 64-65%.

The activity results showed that the most active sample was CNTmox8 and that the activity decreased with the oxidation time, this suggesting that the carboxylic groups play an important role in the reaction. Thus, to verify that the reaction was catalyzed by the carboxylic groups, additional experiments with heat-treated CNToxn24 were performed. Accordingly, two portions of the sample were heated to 373 and 473 K (see Experimental Section for details) and then they were tested on the reaction. The conversion profile, in Fig. 5, shows that while the sample treated at 373 K preserved relatively well the activity compared to CNToxn24, the sample CNToxn24-473 nearly completely lost the activity. These experiments seem to confirm that the oxygen groups responsible of the activity are the carboxylic acids. The importance of Brönsted acid sites on the cyclization of citronellal to isopulegol have already been reported and, for example, over zeolites it was dependent of the number of Brönsted acids [37,38]. The reaction takes place according to the following steps as shown in Fig.7: firstly, the carbonyl group is activated by hydrogen bonding through the interaction with the proton of the surface acid groups. When the carbonyl group is protonated it increases its electrophilicity, this favoring the nucleophilic attack. Then, by intramolecular rearrangement a stable carbocation is formed followed by

deprotonation to obtain isopulegol [36, 38]. Our results show a clear dependence of the activity of the catalysts with the carboxylic acid amount. The catalytic role of carboxylic acid has already been reported in other reactions such as the alcohol dehydration, which was found to be dependent of the amount and accessibility of these oxygen groups [39,40]. Although the role of the carboxylic acids on the catalytic performance of the cyclization of citronellal is clear, it does not follow a linear trend and the activity obtained with CNTmox8 increases by a factor of three compared to CNToxn24. The characterization performed does not suggest any parameter responsible for this higher value. However, some authors suggested that if a marked proportion of oxygen groups are adjacent on the surface, this may negatively affect the adsorption of the reactant by steric hindrance [40].

As long as the selectivity is concerned, the less selective catalysts were CNToxn16 and CNToxn8 which resulted also in the formation of isopulegol ethers. It has been suggested that larger pores favored the formation of dehydration products inside the pores as well as condensation products as diisipulegol ethers [6, 36]. The characterization showed that the oxidation treatment changed the porosity of the samples, this decreasing the pore volume for CNTmox8 and CNToxn24 as a consequence of the agglomeration of the nanotubes. Therefore, a tentative explanation for the higher selectivity obtained with CNTmox8 and CNToxn24 could be that the smaller pore size limited the formation of bulkier molecules.

Conclusions

We have oxidized commercial carbon nanotubes by liquid treatment with H_2O_2 and HNO_3 employing different times and oxidation under air. In addition, one of the samples was ball-milled and then submitted to HNO_3 oxidation. The samples were tested in the

cyclization of citronellal, a reaction which is known to be catalyzed by acids, and their catalytic performances were compared. The characterization studies showed that the samples treated with HNO_3 displayed the largest amount of oxygen on the CNT and that the proportion of carboxylic acids increased with the oxidation time. The sample previously milled had the largest amount of carboxylic acid among the CNT samples which has been ascribed to the creation of more edges on this sample. However, this sample lost surface area during the milling process due to the agglomeration of the nanotubes. The samples treated with air and H_2O_2 presented a low proportion of oxygen and the CNT sample previously milled displayed the highest amount of oxygen among the samples. It was found that only the samples treated in HNO_3 were active on the reaction and the activity was related to the presence of carboxylic acids. The selectivity to isopulegols was high, 97-98%, except for the samples oxidized 8 and 16 hours. This has been ascribed to the different porosity of the HNO_3-treated samples. According to the characterization, for the samples that presented the highest selectivity, the oxidation treatment changed their porosity, reducing the pore volume and this may hinder the formation of secondary products which are bulkier than the isopulegol molecule.

Acknowledgments

Financial support for the present study was received from CONICYT Chile, project 3130483 (Postdoctoral), Generalitat Valenciana, Spain (PROMETEOII/2014/004) is also gratefully acknowledged.

References

[1] E. J. Lenardao, G.V. Botteselle, F. Azambuja, G.Perin, R. G. Jacob, Tetrahedron 63 (2007) 6671–6712.

[2] A.F. Trasarti, A.J. Marchi, C.R. Apesteguía, J. Catal. 247 (2007) 1555-165.

[3] A.F. Trasarti, A.J. Marchi, C.R. Apesteguía Catal. Comm. 32 (2013) 62–66.

[4] Z. Yongzhong, N. Yuntong, S. Jaenicke, G.-K. Chuah, J. Catal. 229 (2005) 404–413.

[5] G.K Chuah, S.H Liu, S Jaenicke, L.J Harrison, J. Catal. 200 (2001) 352–359.

[6] P. Mäki-Arvela, N. Kumar, V.Nieminen, R.Sjöholm, T.Salmi, D.Y. Murzin, J.Catal 225 (2004) 155-169.

[7] F. Rodríguez-Reinoso, Carbon 36 (1998) 159-175.

[8] L.R. Radovic, F. Rodríguez-Reinoso, Carbon materials in catalysis. In: Thrower PA, editor, Chemistry and physics of carbon, (New York: Marcel Dekker, 1997) Vol. 25, pp. 243– 363.

[9] J. L.Figueiredo, M.F.R. Pereira, Catal.Today 150 (2010) 2–7.

[10] J.L.Figueiredo, M.F.R. Pereira in: P.Serp J.L. Figueiredo (Eds.) Carbon Materials for catalysis, John Wiley & Sons, INC, New Jersey, 2009, pp. 177-206.

[11] P. Serp, B. Machado, Nanostructured Carbon Materials for Catalysis, Royal Society of Chemistry, Cambridge, 2015.

[12] R. P. Rocha, J.P.S. Sousa, A.M.T. Silva, M.F.R. Pereira, J.L. Figueiredo, Appl. Catal.B: Environmental 104 (2011) 330–336.

[13] A.G. Gonçalves, J.L. Figueiredo, J. J.M. Órfão, M.F.R. Pereira, Carbon 48 (2010) 4369–4381.

[14] B.Frank, J.Zhang, R.Blume, R.Schlögl, D.Sheng Su, Angew. Chem. Int. Ed. 48 (2009) 6913 –6917.

[15] J.L. Figueiredo, M.F.R. Pereira, M.M.A. Freitas, J.J.M.Orfao, Carbon 37 (1999) 1379-1389.

[16] P.Serp, M.Corrias, P.Kalck, Appl. Catal.A: General 253 (2003) 337–358.

[17] M.L. Toebes, J.M.P. van Heeswijk, J.H. Bitter, A.J. van Dillen, K.P. de Jong Carbon 42 (2004) 307–315.

[18] I.D. Rosca, F.Watari, M.Uo, T.Akasaka, Carbon 43 (2005) 3124–3131

[19] R.R.N. Marques, B.F. Machado, J.L. Faria, A.M.T. Silva, Carbon 48 (2010) 1515 – 1523.

[20] I.Mazov, V. L. Kuznetsov, I.A. Simonova, A. I. Stadnichenko, A.V. Ishchenko, A. I. Romanenko, E. N. Tkachev, O.B. Anikeeva, Appl. Surf. Sci. 258 (2012) 6272– 6280

[21] J. Zhang, H. Zou, Q.Qing, Y. Yang, Q. Li, Z. Liu, X.Guo, Z.Du , J Phys Chem B 107 (2003), 3712–3718.

[22] Moreno-Castilla C, Ferro-Garcia MA, Joly JP, Bautista-Toledo I, Carrasco-Marin F, Rivera-Utrilla J, Langmuir 11 (1995), 4386–4392.

[23] E. Fuente, J.A. Menéndez, D. Suárez, M.A. Montes-Morán, Langmuir, 19 (2003), p. 3505-3511.

[24] I. Tyrone Ghampson, C. Sepúlveda, R.Garcia, L.R. Radovic, J.L. García Fierro, W.J. DeSisto, N.Escalona, Appl.Catal. A: Gen. 439–440 (2012) 111–124.

[25] Z.Wang, M.D. Shirley, S.T. Meikle, R. L.D. Whitby, S.V. Mikhalovsky, Carbon, 47, (2009) 73–79.

[26] Y.Q. Hong, H.P.Xiang, B.Shuo, W. Mao-Zhang, C. Hui-Ming. J. Chem Phys Lett. 345 (2001) 18–24.

[27] B.Xionga, Y.Zhoua, Y.Zhaoa, J. Wanga, X.Chena, R. O'Hayrec, Z. Shao, Carbon 50 (2012) 192–200.

[28] J.P. Tessonnier, D. Rosenthal, T.W. Hansen, C. Hess, M. E. Schuster, R. Blume, F. Girgsdies, N. Pfänder, O. Timpe, D. Sheng Su, R. Schlögl, Carbon 47 (2009) 1779–1798.

[29] A.E. Aksoylu, M. Madalena, A. Freitas, M. Fernando, R. Pereira, J.L. Figueiredo, Carbon 39 (2001) 175–185.

[30] C. Moreno-Castilla, F. Carrasco-Marín, F.J. Maldonado-Hódar, J. Rivera-Utrilla, Carbon 36 (1998) 145-151.

[31] J. L. Figueiredo, M.F. R. Pereira , M.M. A. Freitas , J.J. M. Órfão, Ind ChEng Chem Res, 46 (2007) 4110-4115.

[32] I.Mazov, V. L. Kuznetsov, I.A. Simonova, A. I. Stadnichenko, A.V. Ishchenko, A.I.Romanenko, E.N. Tkachev, O.B. Anikeeva, Appl. Surf. Sci. 258 (2012) 6272– 6280.

[33] F.Liu, X.Zhanga, J.Cheng, J.Tu, F.Kong, W.Huang, C.Chen, Carbon 41 (2003) 2527–2532.

[34] R. Cid, G. Pecchi, Appl. Catal. 14 (1985) 15-21.

[35] A.B. Dongil, B. Bachiller-Baeza, A. Guerrero-Ruiz, I. Rodríguez-Ramos, A. Martínez-Alonso and J. M. D. Tascón. J. Coll. Interf. Sci., 355 (2011) 179-189.

[36] G. D. Yadav, J.J. Nair, Langmuir, 16 (2000) 4072–4079

[37] PJ . Kropp, G.W. Breton, S.L. Craig, S.D. Crawford, J. Org. Chem. 60 (1995) 4146.

[38] M. Fuentes, J. Magraner, C. de las Pozas, R. Rogque-Malherbe, Appl. Catal. 47 (1989) 367

[39] F. Carrasco-Marin, A. Mueden, C. Moreno-Castilla, J. Phys. Chem. B 102 (1998) 9239-9244.

[40] G.S. Szymanski, Z. Karpinski, S. Biniak, A. Swiatkowski, Carbon 40 (2002) 2627-2639.

Figure 1. TEM micrographs of a) CNT, b) CNToxn24, c) CNTmox8.

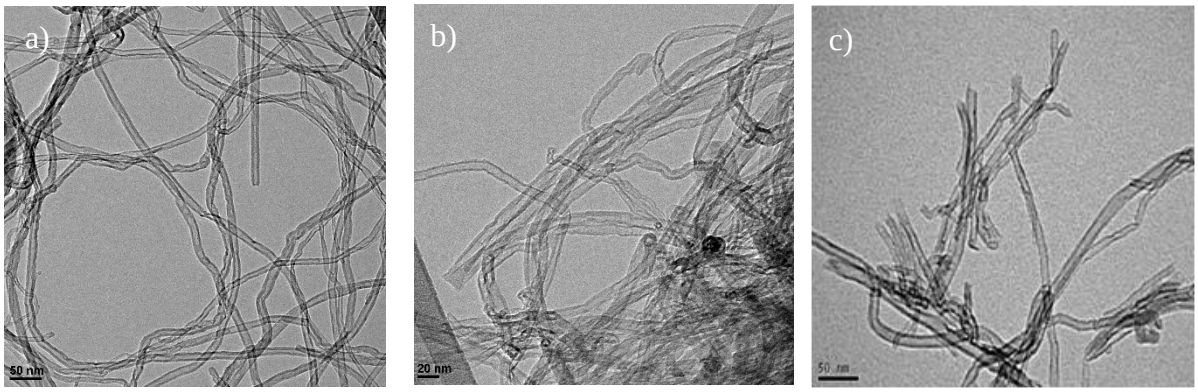

Figure 2. Nitrogen adsorption/desorption isotherms at 77 K of the materials.

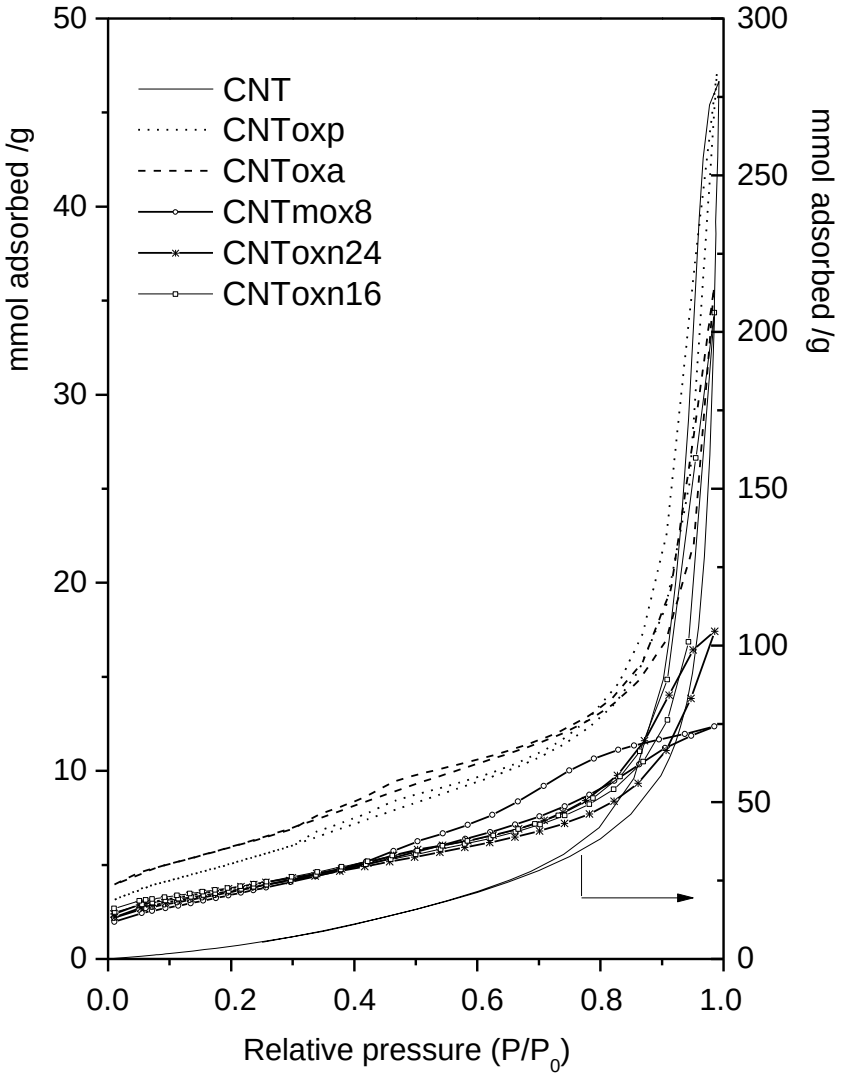

Figure 3. X-ray diffraction patterns of CNT, CNTox24 and CNTmox8.

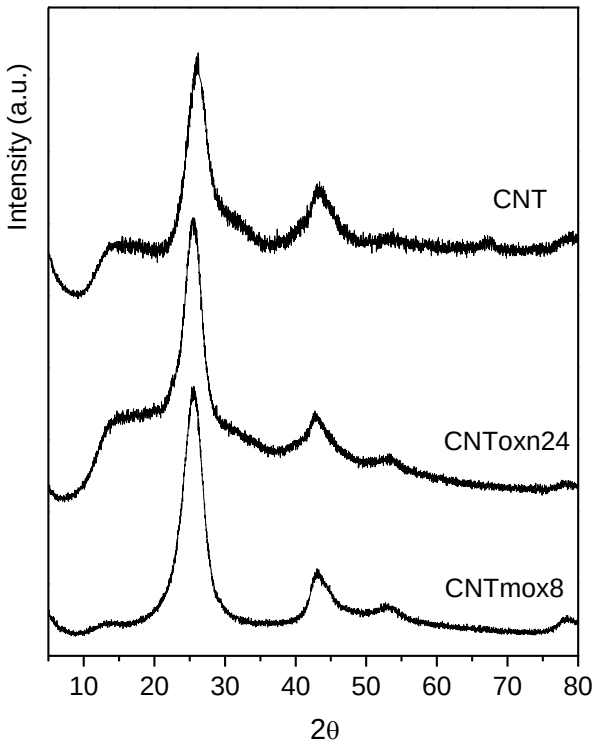

Figure 4. TPD analyses a) CO_2 and b) CO profiles of CNToxn24 (—) CNToxn16 (—○—) CNToxn8 (—) CNTmox8 (----) CNToxp (—x—).

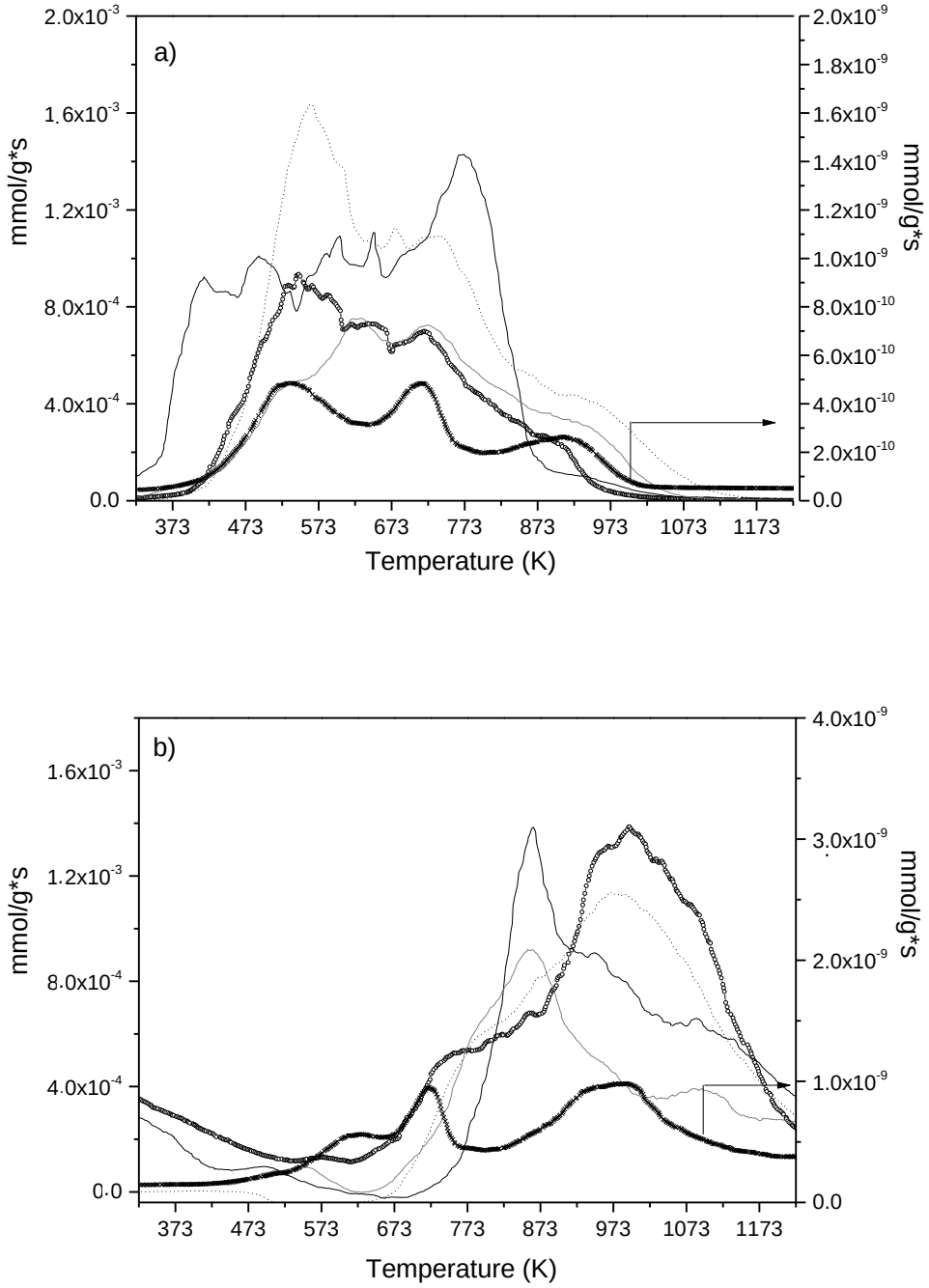

Figure 5. Evolution of conversion of citronellal with time.

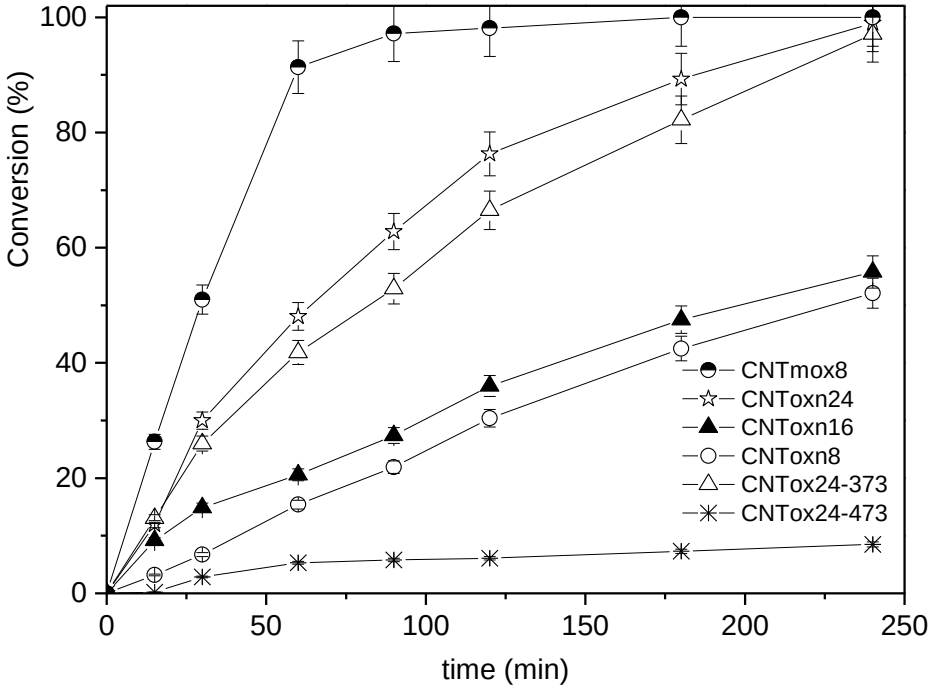

Figure 6. Selectivity to isopulegol *vs* conversion.

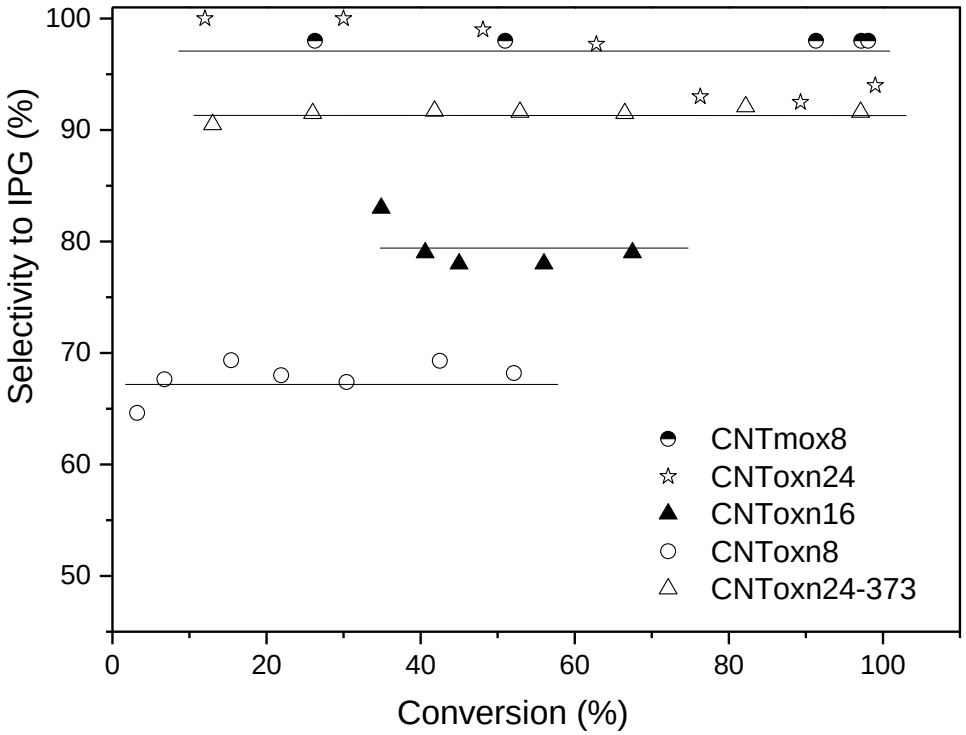

Figure 7. Reaction scheme for cyclization of citronellal [38]

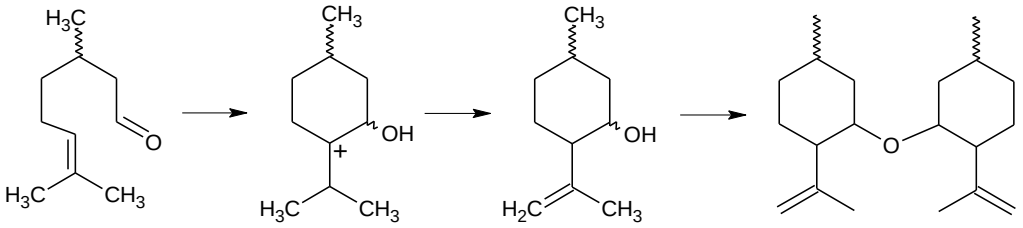

Citronellal Isopulegol Isopulegol ether

Table 1. Textural properties of the materials

Sample	**S_{BET} (m^2/g)**	**V micro (cm^3/g)**	**V meso (cm^3/g)**	**V total (cm^3/g)**
CNT	300	0.01	1.76	1.77
CNToxa	493	0.18	1.46	1.64
CNToxp	463	0.16	1.06	1.22
CNToxn24	295	0.10	0.49	0.59
CNToxn16	310	0.05	1.04	1.09
CNToxn8	289	0.03	1.17	1.20
CNTmox8	301	0.01	0.41	0.42

Table 2. Density of functional groups decomposing as CO_2 and CO estimated by TPD.

Sample	**CO_2 (mmol/g)[a]**	**CO (mmol/g)**	**O (mmol/g)**	**COOH/O**
CNToxp	0.52 (0.13)	0.43	1.5	0.11
CNToxn24	2.77 (0.72)	1.37	6.9	0.10
CNToxn16	1.34 (0.49)	2.51	5.2	0.09
CNToxn8	1.31 (0.29)	1.13	3.7	0.08
CNTmox8	2.89 (1.13)	2.15	7.9	0.14

[a] In brackets, estimated amount of carboxylic acid from the deconvolution of the first peak.

Table 3. Potentiometric results.

Sample	**Acid strength (mV)**	**Total acidity (meq/g)**
CNT	-177	0.08
CNToxa	-133	0.08
CNToxp	293	0.04
CNToxn24	180	0.29
CNToxn16	134	0.27
CNToxn8	87	0.22
CNTmox8	335	0.42

Table 4. XPS atomic surface ratio and oxygen species proportion.

Sample	**O/C**	**O_C=O**	**O_C-O**	**O_COOH**
CNT	0.033	24	57	19
CNToxa	0.043	37	52	11
CNToxp	0.049	24	41	35
CNToxn24	0.090	16	53	31
CNToxn16	0.087	33	50	17
CNToxn8	0.080	49	39	12
CNTmox8	0.089	41	11	48

Table 5. Activity and selectivity to isopulegol.

Sample	**Activity (mmol/g*min)[1]**	**Selectivity to isopulegol[2] (%)**
CNToxa	0.00	-
CNToxp	0.00	-
CNToxn24	0.22	98
CNToxn16	0.13	78
CNToxn8	0.10	69
CNToxn24-373	0.20	92
CNToxn24-473	0.03[3]	-
CNTmox8	0.68	98
CNTmox8-Run2	0.63	97
CNTmox8-Run3	0.60	98

[1] At 50% conversion; [2] At 100% conversion; [3] At 10% conversion